

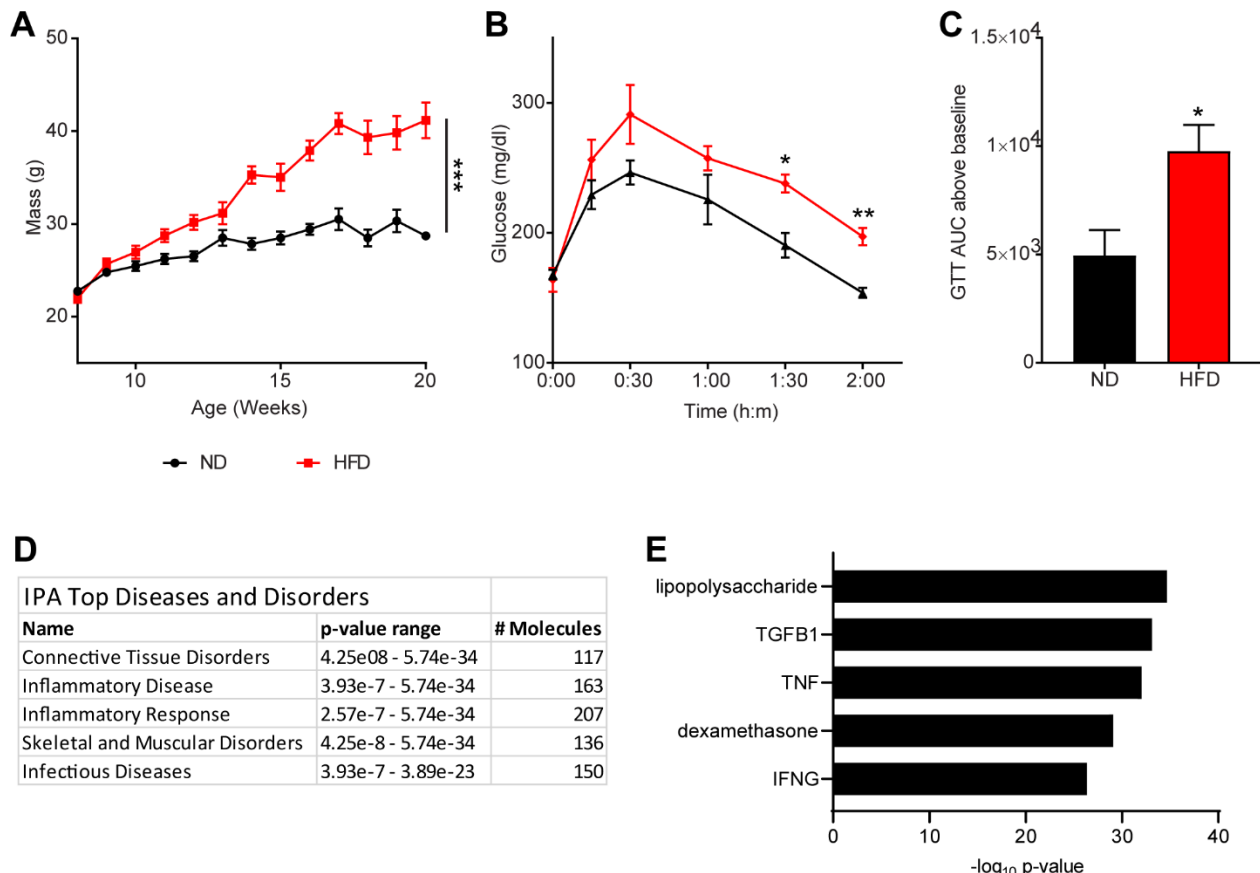
# SUPPLEMENTAL MATERIALS

## A novel long non-coding RNA, MIST, regulates macrophage activation during obesity

Kenneth Stapleton<sup>1, 2</sup>, Sadhan Das<sup>1</sup>, Marpadga A. Reddy<sup>1</sup>, Amy Leung<sup>1</sup>, Vishnu Amaram<sup>1,2</sup>, Linda Lanting<sup>1</sup>, Zhuo Chen<sup>1</sup>, Lingxiao Zhang<sup>1</sup>, Rengasamy Palanivel<sup>3</sup>, Jeffrey A. Deiuliis<sup>3</sup>, and Rama Natarajan\*<sup>1, 2</sup>

<sup>1</sup>Department of Diabetes Complications and Metabolism, Diabetes and Metabolic Research Institute, <sup>2</sup>Irell and Manella Graduate School of Biological Sciences, Beckman Research Institute of City of Hope, Duarte, California; <sup>3</sup>Cardiovascular Research Institute of the Case Western Reserve University, Cleveland, Ohio

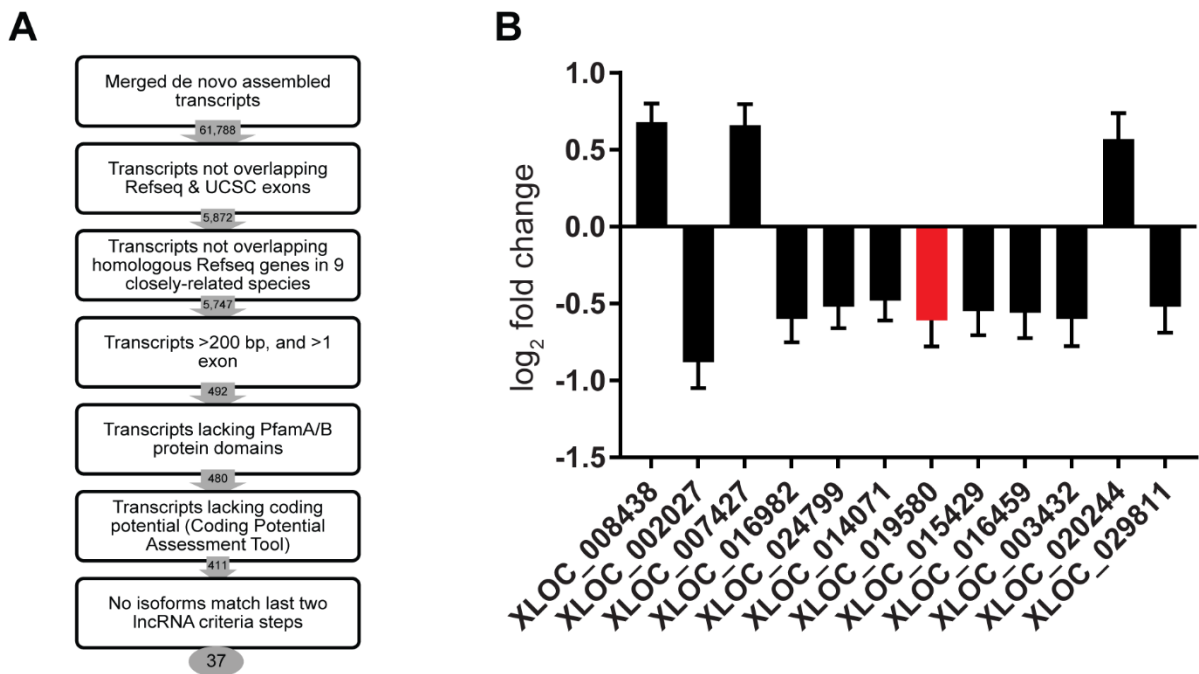
\* Corresponding author



Supplemental Figure I

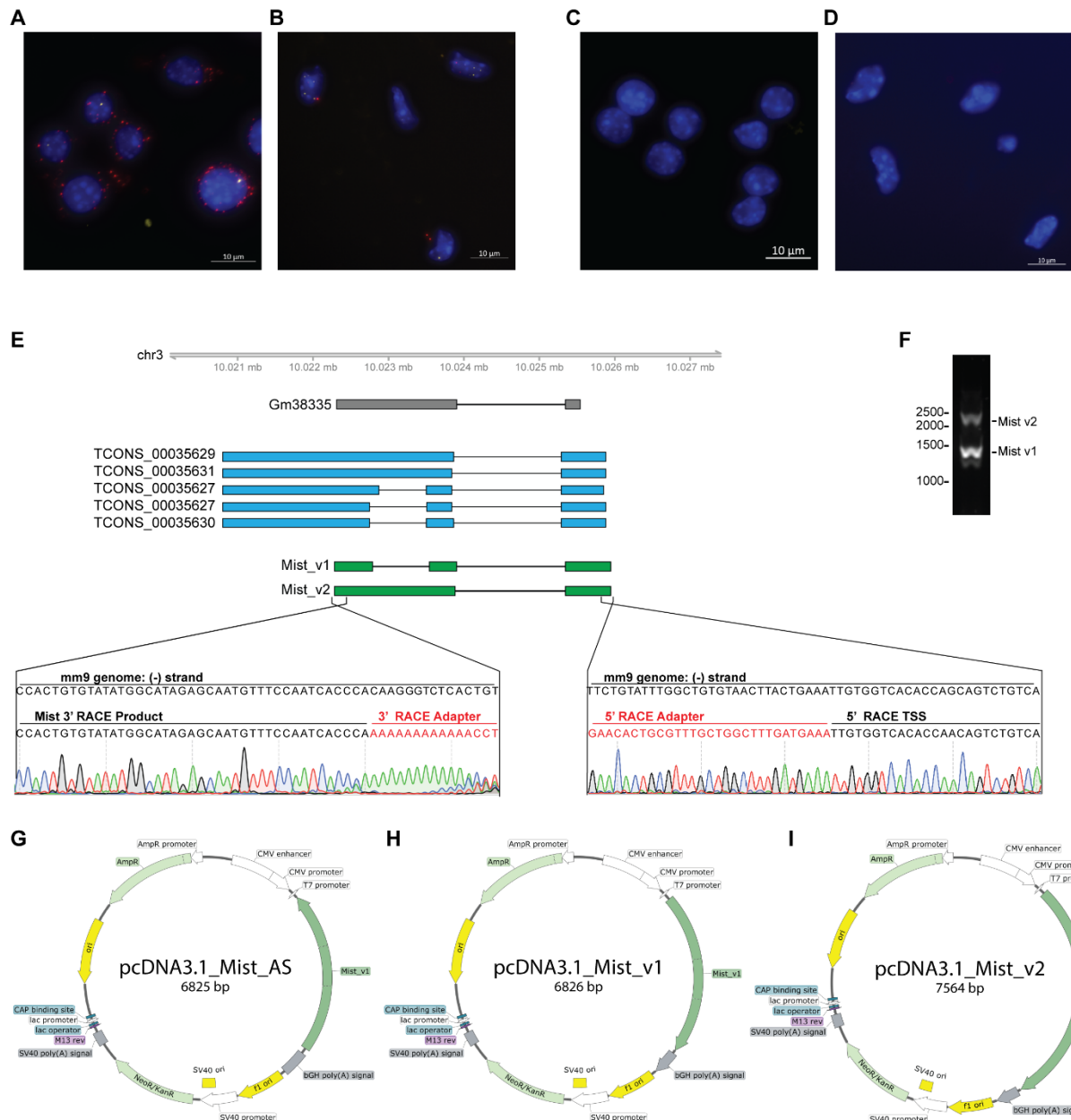
Differential mRNA and lncRNA expression in peritoneal macrophages of high fat diet (HFD) vs normal diet (ND) mice. **(A)** Weight of mice during 12 weeks feeding of HFD or normal diet, beginning at 8 weeks of age. n = 12 mice/group. **(B)** Glucose tolerance test (GTT) in mice after 12 weeks of feeding HFD or normal chow, beginning at 8 weeks of age. Tail vein blood samples were collected at indicated time intervals post injection. n = 12/group. **(C)** Area Under Curve (AUC) analysis of GTT results, normalized by average baseline fasting glucose for each group. **(D)** Ingenuity Pathway Analysis of differentially expressed genes (adjusted p-value < 0.1) based on RNA-seq analysis of elicited peritoneal macrophages (PMs) from HFD-fed mice. **(E)** Top five predicted Upstream Regulators based on p-value, identified using Ingenuity Pathway Analysis.

\*p<0.05, \*\*p<0.01, \*\*\*p<0.001



## Supplemental Figure II

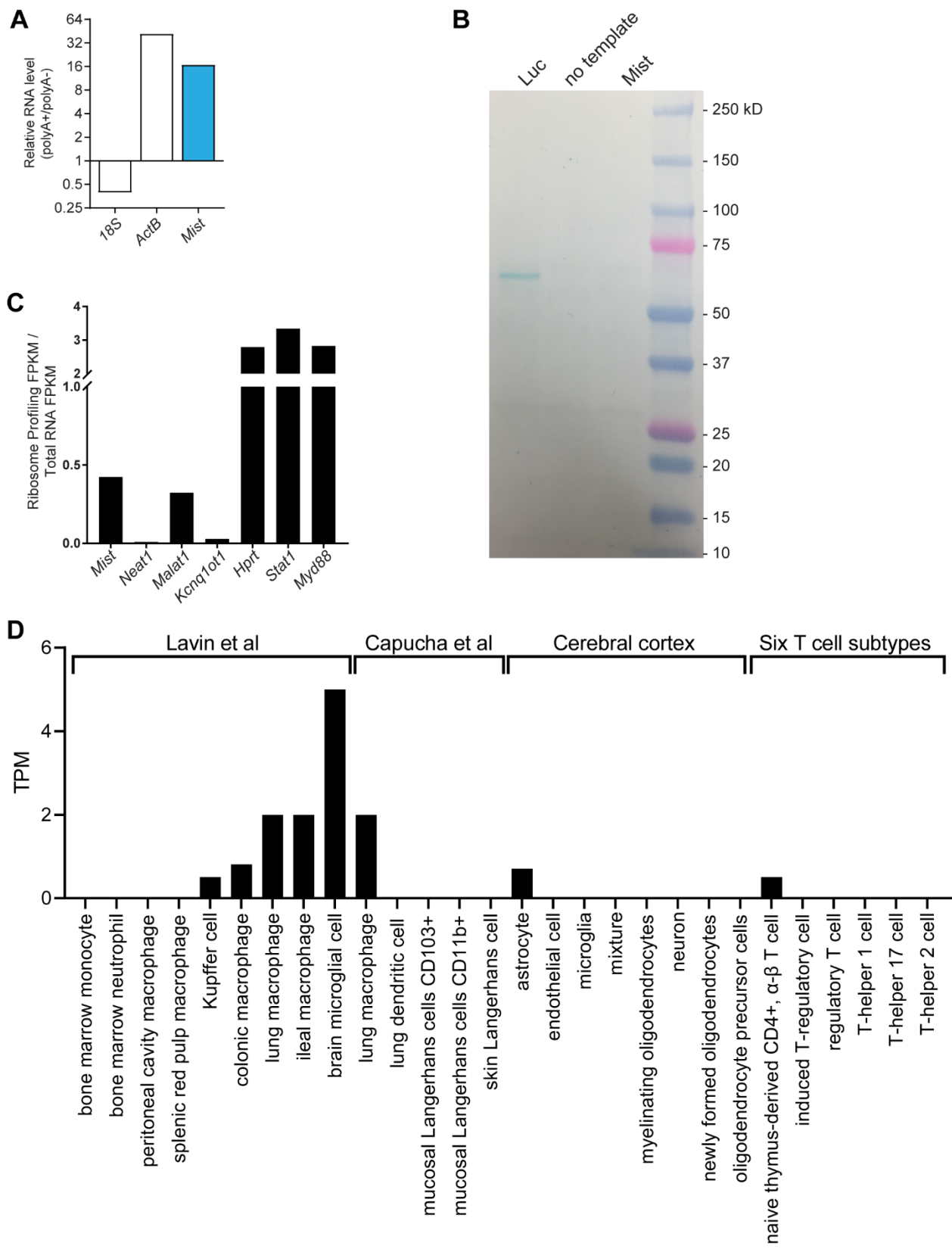
**(A)** Computational pipeline for identification of lncRNAs from *de novo* RNA-seq assemblies. Numbers indicate total *de novo* transcripts that pass each filter. **(B)** Differential expression analysis of novel transcripts identified as lncRNAs from RNA-seq. Transcript XLOC\_019580 was renamed as *Mist* and its function was further characterized. Bars indicate mean + SEM fold change in HFD-fed mouse PMs vs. normal diet.



Supplemental Figure III

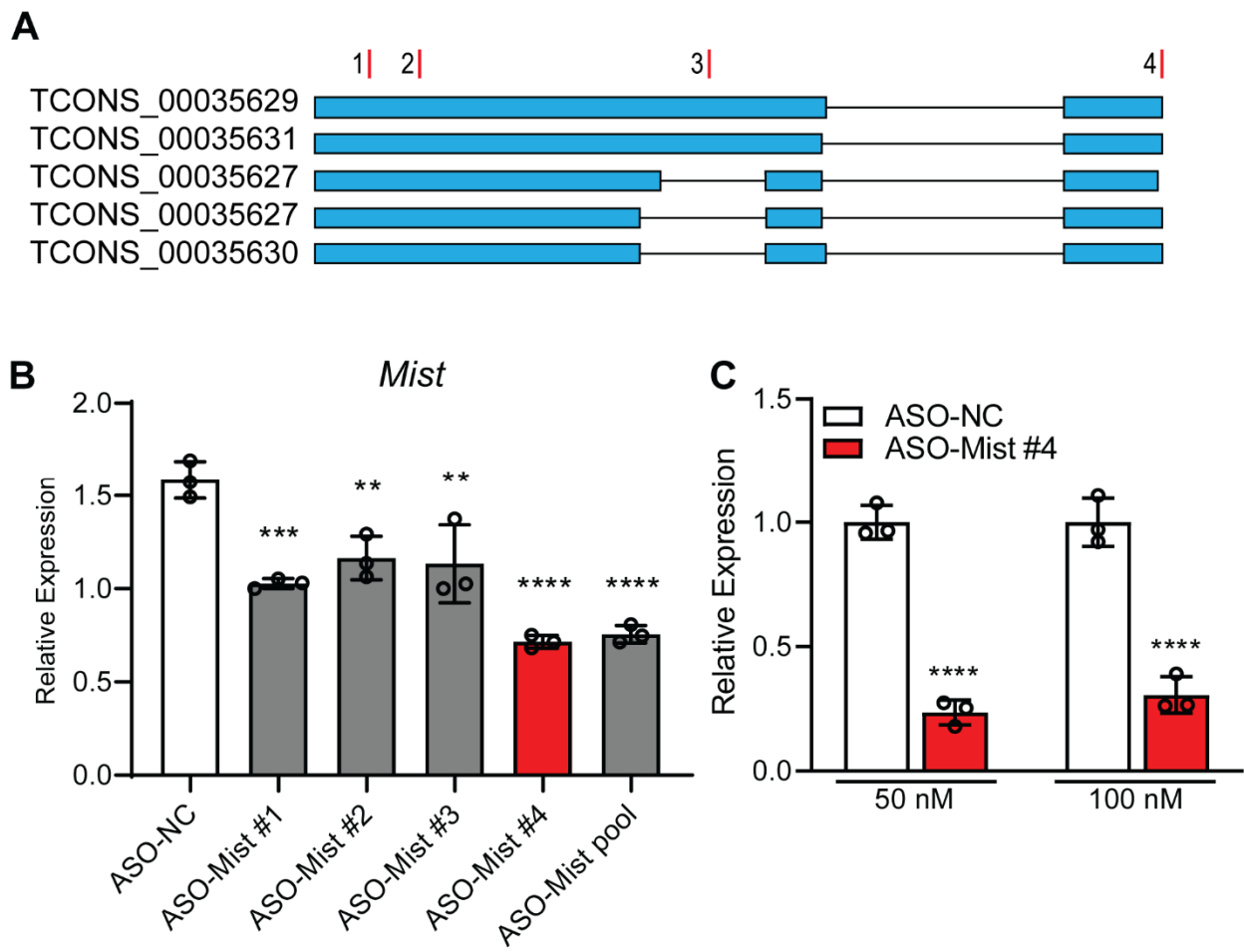
*Mist* characterization and cloning. (A-B) Control images of RNA-FISH in mouse RAW cells (A) and primary PMs (B); related to Figures 1H-I. Probes for *Mist* (yellow) and *Ppia* (red); nuclei are counterstained with DAPI (blue). Scale bars represents 10um. (C-D) Control images for RNA-FISH showing RAW cells (C) and primary mouse PMs (D) treated with no probe but processed through signal amplification steps. Nuclei are counterstained with DAPI (blue). Scale bar represents 10um. (E) Depiction of overlapping transcript predictions at *Mist* locus, including

Genbank mRNA annotation (gray), *in silico* transcript isoform predictions based on RNA-seq data, assembled using Tophat2 software (blue), and *Mist* complete transcripts (green) based on 5' and 3' RACE clones. Sanger sequencing chromatograms of RACE-PCR clones are shown below, aligned to the minus strand of chromosome 3. (F) *Mist* variants, generated using primers targeting 5' and 3' ends of *Mist* and template cDNA from RAW 264.7 cells. (G-I) Plasmid maps of *Mist* splice variants (*Mist\_v1* and *Mist\_v2*) and antisense (*Mist\_AS*) sequence cloned into pcDNA3.1 overexpression vector. To generate AS plasmid, full-length *Mist\_v1* fragment was cloned into pcDNA3.1(-) vector.



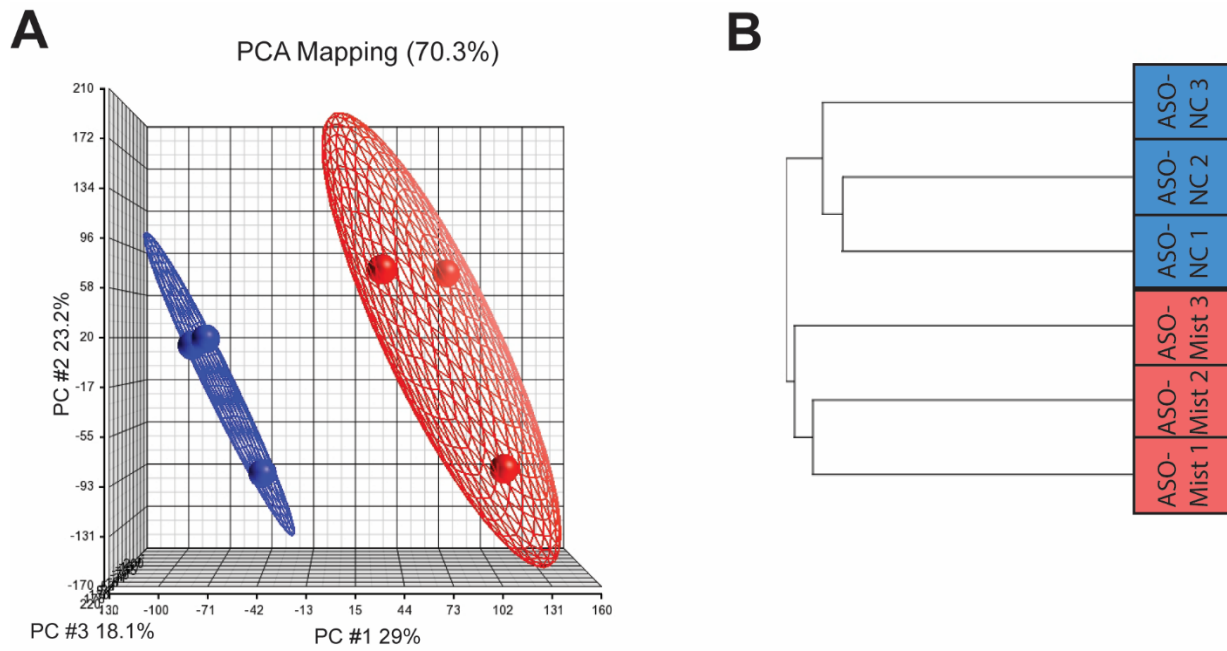
Supplemental Figure IV

Characterization of the *Mist* transcript. **(A)** Ratio of transcript abundance in poly(A)-enriched versus poly(A)-depleted fractions of RNA from mouse PMs. **(B)** In vitro translation assay. Assay was performed using T7 TNT Quick Coupled Transcription/Translation System (Promega) and Transcend Colorimetric Non-radioactive Translation Detection System (Promega) according to manufacturer instructions, using *Mist\_v1* pcDNA3.1(+) construct, as well as T7 Luciferase control DNA as positive control. **(C)** Ribosomal profiling of *Mist* and other lncRNAs and mRNAs. Bars represent ratios of fragments per transcript killobase per million reads (FPKM) from global ribosomal profiling vs. total RNA-seq in mouse PMs. Raw data from Wang et al<sup>1</sup> was aligned to mm9 genome assembly using HISAT2 and gene FPKM values were generated using Cufflinks. **(D)** Transcript per million read (TPM) values from baseline cell type RNA-seq experiments in the EMBL-EBI Expression Atlas database. Among the 36 RNA-seq sets FOR *Mus musculus* in the database, expression of Gm38335 was detected among 4 datasets (top labels) and mostly enriched in macrophages.



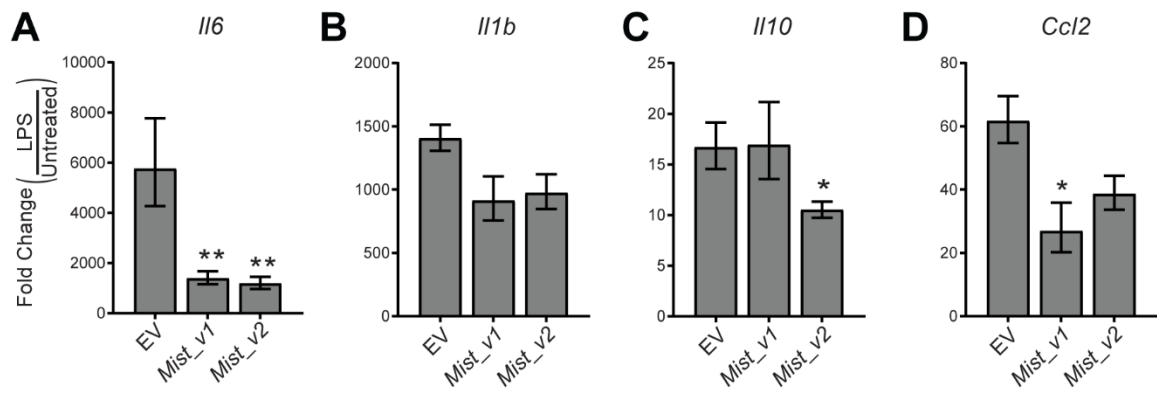
Supplemental Figure V

Design and efficacy of LNA-modified antisense oligonucleotides (GapmeRs) targeting *Mist*. (A) Four GapmeRs were designed to target various regions of *Mist* *in silico* predicted transcripts. (B) RT-qPCR analysis of *Mist* expression in RAW cells 48 h post-transfection of *Mist*-targeted GapmeRs (ASO-Mist) or non-targeting GapmeR (ASO-NC) at 100nM. Individual GapmeRs and pooled GapmeRs were tested for *Mist* silencing efficacy. ASO-Mist #4 was most effective, and was used for subsequent knockdown experiments. n = 3. (C) Optimization of transfection conditions showed greatest knockdown efficacy at 50nM GapmeR concentration. n = 3. Data are presented as mean ± SD. \*\*p<0.01, \*\*\*p<0.001, \*\*\*\*p<0.0001, calculated using One-Way ANOVA followed by Dunnett multiple comparisons test (B) or student's t-test (C).



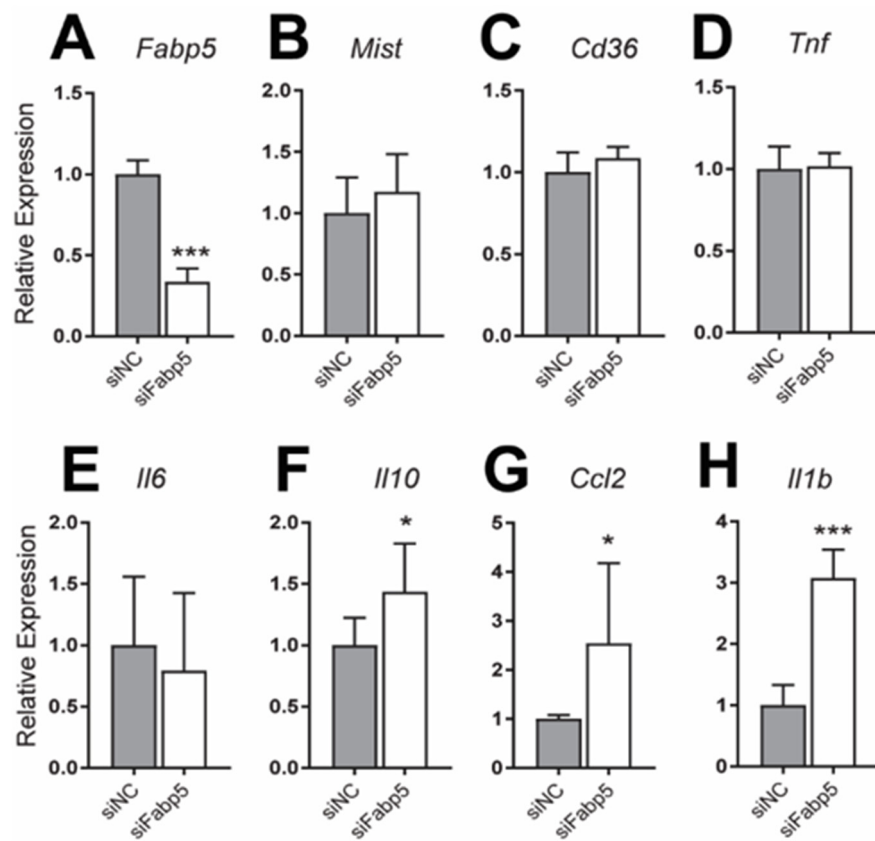
Supplemental Figure VI

Batch analysis of GapmeR-mediated knockdown followed by microarray analysis. (A) Principal component analysis of *Mist*-targeted GapmeR (red) and negative control GapmeR (blue). (B) Hierarchical clustering of samples. Both visualizations were generated using Partek software. Information on GapmeR design and selection can be found in Supplemental Figure 5.



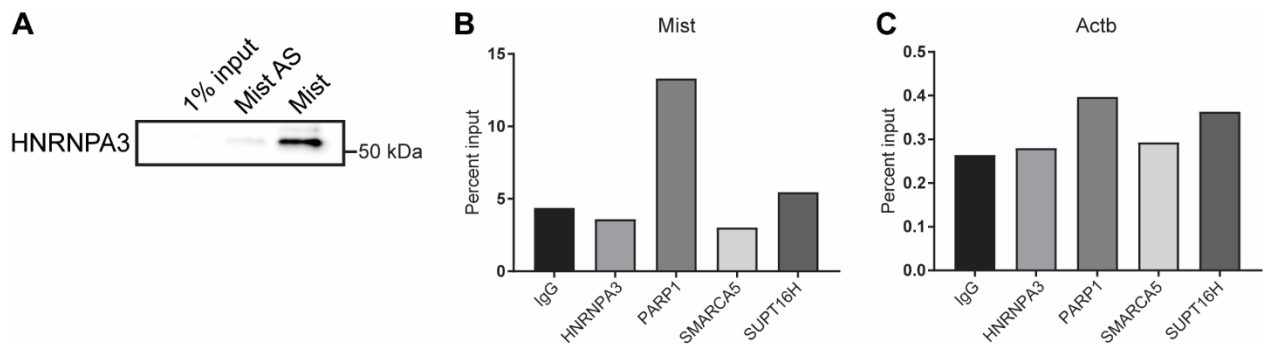
Supplemental Figure VII

**(A-D)** RT-qPCR of LPS-induced gene expression, fold change relative to untreated cells after transient *Mist* overexpression in RAW cells for 72h. Bars represent mean  $2^{-\Delta\Delta Ct}$  values, error bars represent SEM. n=3. \*p<0.05, \*\*p<0.01



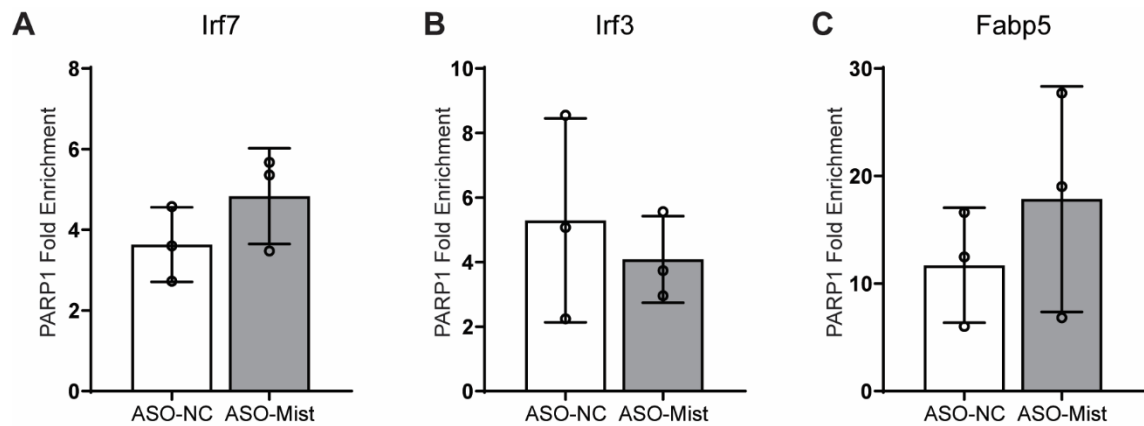
Supplemental Figure VIII

Effects of siRNA-mediated silencing of *Fabp5*. (A) – (H): RT-qPCR of indicated genes after transfection with ON-TARGETplus *Fabp5*-siRNA pool (siFabp5) or non-targeting control (siNC) siRNA (both manufactured by Dharmacon); n=6 except for *Il6* and *Tnf* (n=3). Bar graphs represent mean values, error bars = SEM. \*p<0.05, \*\*\*p<0.001



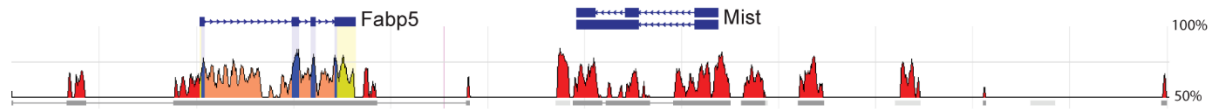
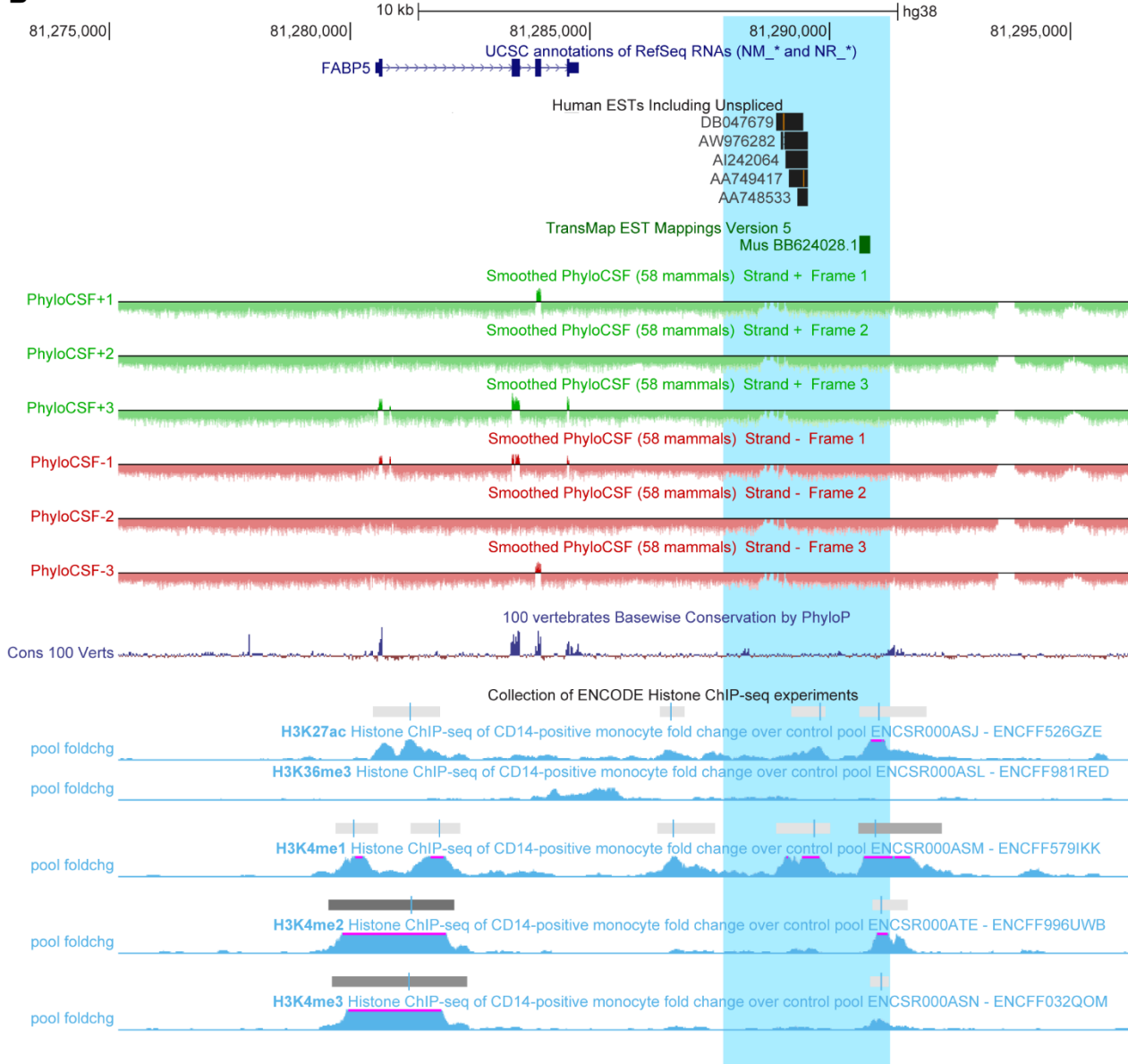
Supplemental Figure IX

(A) RNA-pulldown followed by Western blot using HNRNPA3 antibody. RNA-protein complexes were run on SDS-PAGE gel and probed using HNRNPA3 antibody. (B) Native RNA Immunoprecipitation (RIP) of candidate Mist-interacting candidate proteins. HNRNPA3, PARP1, SMARCA5 and SUPT16H were immunoprecipitated from RAW nuclear lysates, and *Mist* (**B**) and *Actb* (**C**) RNA was measured by qRT-PCR. IgG was used for isotype-control IP.



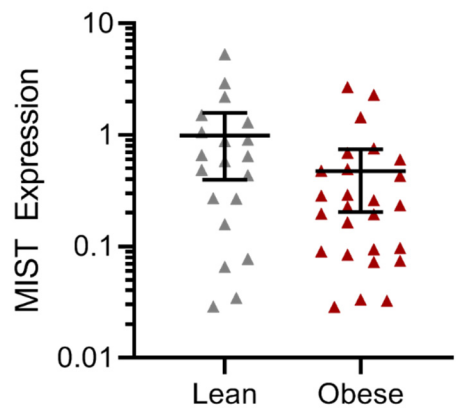
Supplemental Figure X

**(A-C)** Associated with Figure 5E, ChIP-qPCR for PARP1 enrichment at promoters of indicated genes. ChIP assay was performed using PAR-optimized protocol (see Methods). n=3 per group.

**A****B**

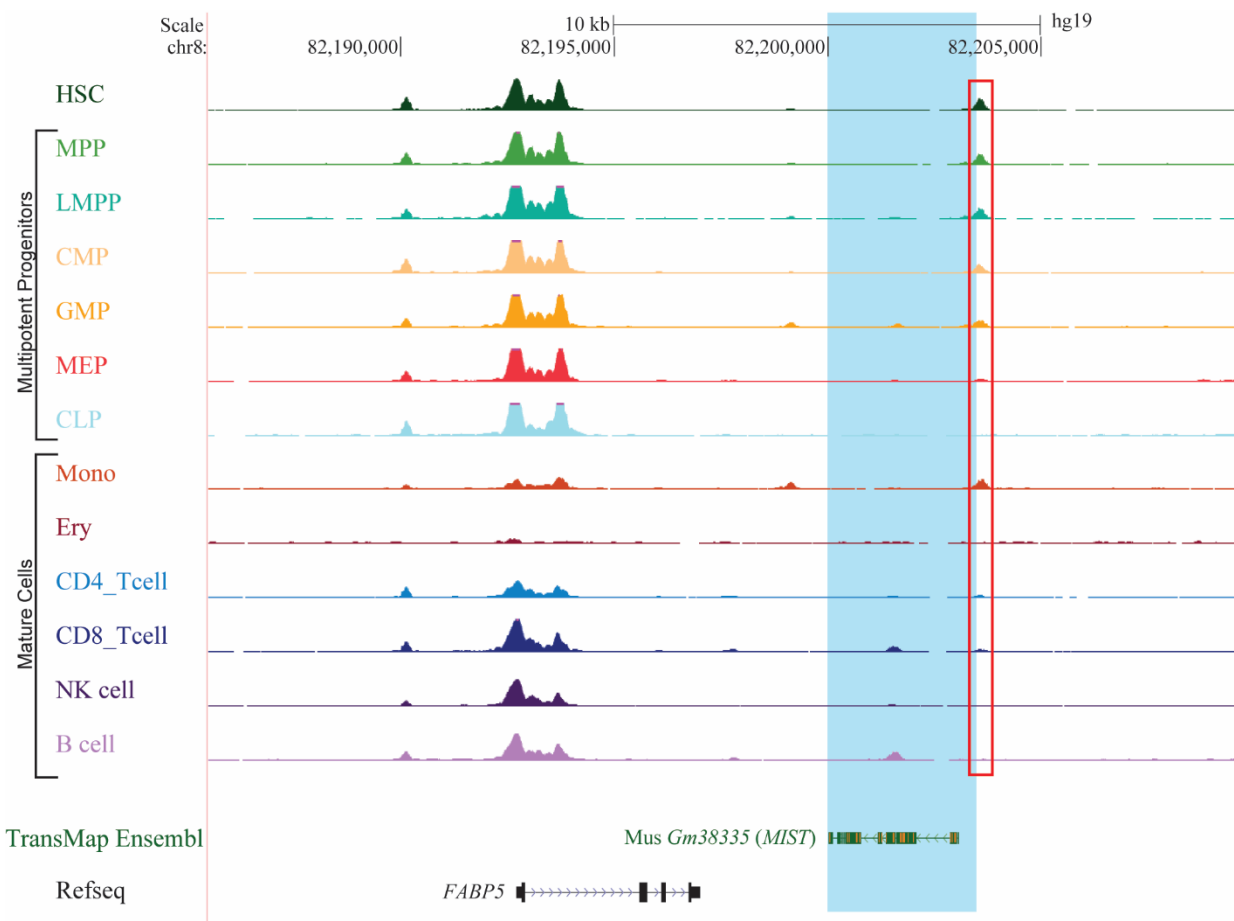
Supplemental Figure XI

Evidence of *Mist* homology in humans. (A) Evolutionarily conserved domains within *Mist* genomic locus between mouse (mm9) and human (hg19) genome assemblies. Peak height represents degree of homology in human genome compared to mouse. X-axis represents mm9 chr3:10005000-10035000. Peak colors indicate relation to protein-coding features within the conservation profile; blue corresponds with coding exons, yellow with UTRs, salmon with intronic sequences and red with intergenic sequences. Tracks were generated with ECR Browser<sup>2</sup>. (B) Snapshot of *Fabp5-Mist* locus from hg38 UCSC Genome Browser. Light blue box represents predicted *Mist* locus, determined using LiftOver tool. ESTs and Human ESTs overlapping *Fabp5* were removed.



Supplemental Figure XII

*MIST* expression in stromal vascular fraction (SVF) of adipose tissue samples from obese and lean donors. Adipose tissue was collected from obese patients undergoing bariatric surgery and lean donors. Brackets represent mean  $\pm$  95% CI.  $p=0.08$ .



Supplemental Figure XIII

Chromatin accessibility at human *MIST* locus at various stages of hematopoietic differentiation. Normalized ATAC-seq tracks generated from 13 cell populations from various stages of human hematopoietic hierarchy. Tracks and figure were adapted from Corces et al<sup>3</sup>. Blue highlight shows *MIST* locus determined by Lift-over tool in UCSC Genome Browser. Red box indicates putative *MIST* promoter. HSC, hematopoietic stem cells; MPP, multipotent progenitor cells; LMPP, lymphoid–primed multipotent progenitor cells; CMP, common myeloid progenitor; GMP, granulocyte–macrophage progenitor cells; MEP, megakaryocyte–erythroid progenitor cells; CLP, common lymphoid progenitors.

**Supplemental Table I** – Clinical characteristics of lean, obese healthy, and obese unhealthy subjects

Characteristics	Lean (n=20)	MHO (n=6)	MUO (n=20)
Female	10/20 (50)	5/6 (83)	12/20 (60)
BMI (kg/m <sup>2</sup> )	26.2 ± 2.0	45.9 ± 4.8	53.4 ± 8.6*
Fasting Glucose (mg/dL)	100.3 ± 11.6	84.5 ± 18.0	93.3 ± 11.3
Fasting Insulin (mIU/mL)	7.42 ± 5.18	7.05 ± 2.17	21.89 ± 21.56†
Total Cholesterol (mg/dL)	188 ± 35	145 ± 43	168 ± 52
Triglyceride (mg/dL)	116.1 ± 74.2	74.3 ± 37.4	127.2 ± 76.4
HDL (mg/dL)	45.0 ± 9.1	38.2 ± 15.5	39.0 ± 7.8
LDL (mg/dL)	120.3 ± 31.2	91.8 ± 38.4	106.7 ± 35.0
HbA1c % (mmol/mol))	5.09 ± 0.31 (32)	4.92 ± 0.43 (30)	5.41 ± 0.56 (36)
CRP (mg/dL)	4.22 ± 4.50	12.14 ± 9.76	10.63 ± 8.73
HOMA-IR	1.95 ± 1.33	1.45 ± 0.53	5.12 ± 5.40†
QUICKI	0.364 ± 0.045	0.365 ± 0.020	0.314 ± 0.026†

Data are mean ± SD, or n (%). MHO, Metabolically healthy obese; MUO, Metabolically unhealthy obese; CRP, C-reactive protein; QUICKI, quantitative insulin-sensitivity check index. MHO cohort was defined as BMI > 40 and the following criteria: Triglyceride < 150 mg/dL, Fasting glucose < 101 mg/dL, Fasting insulin < 10 mIU/mL, and HbA1C < 5.7%. MUO cohort was defined as all obese subjects (BMI > 40) who failed to meet MHO criteria. HOMA-IR was calculated using the following equation: [glucose (mg/dl) x insulin (mIU/L)/405]. QUICKI was calculated using the following equation: [1/(log(insulin(mg/dl)) + log(glucose(mg/dl))]. \*p < 0.05, †p < 0.001 comparing MHO to MUO subjects.

**Supplemental Table II** – Primer and GapmeR sequences used in this study

Mouse qPCR primers	Forward	Reverse
<i>Actb</i>	AGGAGTACGATGAGTCCGGC	GGTGTAAAACGCAGCTCAGTA
<i>Fabp5</i>	TGGCAACAACATCACGGTCA	GGTCAGACCGTCTCAGTT
<i>Mist</i>	ACAAGGCTACCTCTGTCGCT	GATCTCCAGCAGGCGAAAAC
<i>Ppard</i>	TCACCAGCAGCCTAAAGCA	AGGCCAGGCTTCTGGAAAG
<i>IL18</i>	TCTTGGCCCAGGAACAATGG	ACAGTGAAGTCGCCAAAGT
<i>Srebp1</i>	CTTTCCCTAACGTGGGCCT	TCAAACCGCTGTGTCCAGT
<i>IL1b</i>	TGCCACCTTTGACAGTGATG	TGATGTGCTGCTGCGAGATT
<i>Ifng</i>	TTCAGCAACAGCAAGGCGAA	ATTGAATGCTGGCGCTGGA
<i>Cd97</i>	CCATGAGGGGCGTCAGATG	GCACAGTTCTTACTCTGCCT
<i>Ccl2</i>	AGGTCCCTGTATGCTTCTGG	CAGCACTTCTTGGGACACCTGCTG
<i>Cd36</i>	GATGACGTGGCAAAGAACAG	TCCTCGGGTCCTGAGTTAT
<i>Il6</i>	ACAAAGCCAGACTCCTCAGAG	ACCACAGTGAGGAATGTCCAC
<i>Il10</i>	TGCTTCTATGCAGTTGATGAAGAT	AGCTCCAAGACCAAGGTGTC
<i>Nos2</i>	CCTGGAGACCCACACACTGG	CACAGCCACATTGATCTCCG
<i>Tnf</i>	TGTTGCCTCCTCTTGCTT	TGGTCACCAAATCAGCGTTA
<i>Arg1</i>	TGCATATCTGCCAAAGACATCG	CGTAGAAGTGTCCCCAGGGTCTACG
<i>Cd206</i>	GTGGAGTGATGGAACCCAG	CTGTCGCCAGTATCCATC
<i>Il4</i>	TCCATTGCATGATGCTTT	AGCTGCACCATGAATGAGTC
Human qPCR Primers	Forward	Reverse
<i>ACTB</i>	ATGATGATATGCCCGCGCTC	AATCCTTCTGACCCATGCC
<i>FABP5</i>	ACAATGTCACCTGTACTCGGA	AGAAACAGTATGGAGATTGCTCA
<i>MIST</i>	TCACTGCCATTGATGGTCA	AAACCAGTTCACCGGCTTCA
<i>GAPDH</i>	CATCACTGCCACCCAGAAGACTG	ATGCCAGTGAGCTCCGTTCA
ChIP qPCR	Forward	Reverse
Tnf_pro	CCCAAGGGCTATAAAGGCGG	CTGGCTAGTCCCTGCTGTC
Irf7_pro	GTGAAAAGGAGGGTGCAGT	ACACCCTAGTGACGTCTGGA
CD36_pro	GCTAGGAAACCATCCACCACT	GCTCGTTCAACTCTCACACAC
Irf3_pro	AGAAGGCTCGAAGACCGTAG	AAAGTGGGAAATCGGACCAAG
Il6_pro	AGTGCTCATGCTTCTAGGGC	TGTGACGTCGTTAGCATCG
Fabp5_pro	CAGCTGCACTAAGGGAGGC	GGACTGGACGTACGTTT
Other primers	Forward	Reverse
mMist full sequence	TTGTGGTCACACCAACAGTCT	GGGTGATTGGAAACATTGCTC
GapmeRs		
Mist GapmeR#4	TATGACAGACTGCTGG	

**Supplemental Table III** – HFD-induced differentially expressed novel lncRNAs and nearest neighboring gene

Gene	Log <sub>2</sub> Fold Change (HFD/SD)	Adjusted p-value	Nearest known gene	bp to coding gene	Log <sub>2</sub> Fold Change	Adjusted p-value
XLOC_008438	0.68	5.44E-06	<i>Gm2848</i>	8120	0.435	0.148
XLOC_002027	-0.88	4.25E-05	<i>Pde7b</i>	0	-0.571	0.019
XLOC_007427	0.66	2.65E-04	<i>Klf6</i>	-16021	0.119	0.667
XLOC_016982	-0.60	4.99E-03	<i>Ovol2</i>	-5331	-	-
XLOC_024799	-0.52	1.05E-02	<i>Dnah6</i>	0	-	-
XLOC_014071	-0.48	1.14E-02	<i>Impact</i>	3282	-0.242	0.247
XLOC_019580 <i>(Mist)</i>	-0.61	1.39E-02	<i>Fabp5</i>	-5696	-0.374	0.018
XLOC_015429	-0.55	1.99E-02	<i>Npas4</i>	-218	-0.232	0.605
XLOC_016459	-0.56	2.24E-02	<i>Agps</i>	48762	0.071	0.823
XLOC_003432	-0.60	2.71E-02	<i>Lta4h</i>	181	-0.163	0.551
XLOC_020244	0.57	3.12E-02	<i>Bcar3</i>	27785	0.202	0.506
XLOC_029811	-0.52	5.53E-02	<i>Mir21c</i>	72401	-	-

High fat diet-responsive novel lncRNAs identified in mouse PMs, paired with the most proximal gene and respective change in expression upon HFD. Neighboring genes were identified using “nearest” command from bedtools software. Highlighted row corresponds to *Mist* and *Fabp5*.

**Supplemental Table IV – Mist isoform sequences, cloned from RAW264.7 cDNA**

>Mist\_v1  
TTGTGGTCACACCAACAGTCTGTCATAAAAGGAGTCTTGTCTCTGGAGCTTCCAAACTTCTATGTGA  
ATGTCATTGCTACTAGTTGAAGCTCTGAAATCCATCTGGAAATTCCTTCTTGTATTTGTTCT  
TTCAGTAATAGTCTAGATAAAAAAGTCAAGAAGCTAACGAGATATAAACAAACAATAACAACAAAA  
AAGTGCCAGGGCTTCAGAGACCTCACACATGGTACCCACAACCTGGTATGCCATGCACATGGAAGACGGAG  
AAGAAGGCACTGGCTTGTGCCTAACGAAATTCAAGGTTACGTAACTCGGTGACAAAGAAAGAACCTC  
CACTATAAAACAGACATCAATTCTTAACGTAGAATAATGATTCCCCGATCCAGATGTTGATGTGCAA  
GGGAAAGATGTGATCCCTGCTAGTAAACTGCCTGCTGGGGAAACCATTGTGCAACATAGAACGCTCC  
GGTACCAACACATCCATTGTACAAGGCTACCTCTGCGCTGCCCTCATGTGAGCTGCTGTGTTGAAA  
ACTGGCAGAAGCAGCCTCCCCAGCAAGTTTCGCCTGCTGGAGATCTGCTCTGAGACAAATATAGAGGATGGA  
GACGTTTGTGGCTTGTGCCATCAAAGACCAATTGCTTGCAGGAAATGAAGTGCAGCCTCT  
GCCCGTCCACCTCCACAAGTACTGTCAAGTGAGAACAGCTGAAGCAGTTGACTGAGTTCCC  
TCTGAGCCAATTCAAAGCTCACAAATGTCAATTAAACCACCAAGTACTTGGAGGAGAGCTTAA  
AGTACTTTCAAAGAGAGTTCTAGGAAGAGCTATTCAAATATCAGTCTGTCAATTTCACCAC  
GGGAAAGATGTGATCCCTGCTAGTAAACTGCCTGCTGGGGAAACCATTGTGCAACATAGAACGCT  
GGTACCAACACATCCATTGTACAAGGCTACCTCTGCGCTGCCCTCATGTGAGCTGCTGTGTTGAAA  
ACTGGCAGAAGCAGCCTCCCCAGCAAGTTTCGCCTGCTGGAGATCTGCTCTGAGACAAATATAGAGGATGGA  
GACGTTTGTGGCTTGTGCCATCAAAGACCAATTGCTTGCAGGAAATGAAGTGCAGCCTCT  
GCCCGTCCACCTCCACAAGTACTGTCAAGTGAGAACAGCTGAAGCAGTTGACTGCT  
TCTGAGCCAATTCAAAGCTCACAAATGTCAATTAAACCACCAAGTACTTGGAGGAGAGCTTAA  
AGTACTTTCAAAGAGAGTTCTAGGAAGAGCTATTCAAATATCAGTCTGTCAATTTCACCAC  
ATCGGGGtttgtttgtttgtttgtttgtttgtttatGAACAGGCACCTCTCACTCCTAGC  
TGATACCCCTGGTGGTGTCACTGACCTTCAGATTCCACGTTCTCCTGAACAAGTACAGAGCCACGTGCTG  
TGCTCCCTGCTCAAGTCTTAGACAGTTGCCCTGCATTGCTTCTTTTCCATTGATTAATTATTAC  
TACTTACATCTGGATGAATCATATcctcccttctctctcccccagccctccctcc  
ccccctccacacccctccAAAGCTTATCATCTGTGGCTCCCTGTCCCCATCTGGGCTCTGCC  
TCTTGTCACTTACAATACACTAGACTCAGATATTGcctgactaccctgatcatcact  
tatgaccttgagagagccctccatctcatcgtagttccctatgc  
GGTTGGGTTGCTTCCCAGCTGTGCACTCCCTAGGCTGAGCCTTGACCTGTATGTTCTATCTCC  
TCACTCTAGTGTCACTCCAGGAGAAAGACCCCTGCCCTATCTGCCCTGCTCTGGCTGCTTAAATTGCTC  
TTTGTGTTATACACTGCTGTGACTAAAAAAAAAAATCATTCCAAAGACACTTCTGTTCCCAGAAATT  
TAAAGTGTGCACTGCAGGAAGAGACAGGAAGAAGAGGACTGGATTGAAAGAGAAATGGTCC  
TGACAGAGCCGGACAGAGCAGATGTCAAGACTCCAGTTATTTCAGCTCTGGTGTGACAGTGGTGTGACCA  
GCAGCCAGTCATACCACCCCTGCCCTCACACCTGAAGAGACACGTCACTCAGCTCTAA  
GCTTCATCAGTCCAGCACACAAGAGCATCTAACGAGCAGTCAACAGAGCTGAGAGAAAT  
AAACAACAAAAACTAGGAGAAAGCTGTAAATTCTCCTAAGTCAACAGACAATGCA  
TTAAAAACAGTAAGCAGTGGGTTTGAGAAAACAGCTGATGACCTTAAGAATCAAGAAAGCATGT  
GACAAATA  
GACGAAATAGAACCAACTGTGATATGGCATAGAGCAATGTTCCAATCACC  
AAAAAA

**Supplemental Table V – Complete List of Mass Spectrometry results for RNA Pulldown**

Identified Proteins	Accession Number	Number of Peptides	
		Mist AS	Mist
poly [ADP-ribose] polymerase 1 (PARP1)	NP_031441.2	3	60
PREDICTED: heterogeneous nuclear ribonucleoprotein L isoform X2	gi 568944892	4	62
ATP synthase subunit beta, mitochondrial precursor	NP_058054.2	2	27
nucleolar RNA helicase 2	NP_062426.2	3	39
PREDICTED: heterogeneous nuclear ribonucleoproteins A2/B1 isoform X1	gi 755517050	4	46
polyadenylate-binding protein 1	NP_032800.2	2	20
ATP synthase subunit alpha, mitochondrial precursor	NP_031531.1	3	28
heterogeneous nuclear ribonucleoprotein A3 isoform a (HNRNPA3)	NP_932758.1	5	44
heterogeneous nuclear ribonucleoprotein A1 isoform b	NP_001034218.1	4	35
myosin-9 isoform 1	NP_071855.2	2	16
nucleophosmin isoform 1	NP_032748.1	4	32
myb-binding protein 1A	NP_058056.2	5	31
60S ribosomal protein L7a	NP_038749.1	2	12
nucleolin	NP_035010.3	12	63
60S ribosomal protein L4	NP_077174.1	8	40
N-acetyltransferase 10	NP_694766.1	2	10
40S ribosomal protein S3a	NP_058655.3	4	19
PREDICTED: rRNA 2'-O-methyltransferase fibrillarin	gi 568889938	3	14
78 kDa glucose-regulated protein precursor	NP_001156906.1	6	26
lipoamide acyltransferase component of branched-chain alpha-keto acid dehydrogenase complex, mitochondrial	NP_034152.2	3	13
60S ribosomal protein L7	NP_035421.2	4	17
PREDICTED: 40S ribosomal protein S6	gi 755501126	3	12
aldehyde dehydrogenase, mitochondrial precursor	NP_033786.1	3	12
40S ribosomal protein S8	NP_033124.1	5	19
probable ATP-dependent RNA helicase DDX17 isoform 1	NP_951062.1	4	15
heterogeneous nuclear ribonucleoprotein U-like protein 2	NP_001074665.1	12	42
RNA-binding protein 14	NP_063922.2	8	28
heterochromatin protein 1-binding protein 3 isoform 1	gi 550821838	2	7
serine/arginine-rich splicing factor 7 isoform 1	NP_666195.1	2	7
60S ribosomal protein L10a	NP_035417.2	2	7
probable ATP-dependent RNA helicase DHX37	NP_976064.1	2	7
PREDICTED: RNA binding motif protein, X-linked-like-1 isoform X1	gi 568956346	7	24
plectin isoform 12alpha	NP_001157012.1	86	287
PREDICTED: acetyl-CoA carboxylase 1 isoform X3	gi 568971082	3	10
heterogeneous nuclear ribonucleoprotein U	NP_058085.2	29	96
guanine nucleotide-binding protein-like 3 long isoform	NP_705775.2	5	16
PREDICTED: probable ATP-dependent RNA helicase DDX5 isoform X1	gi 568971472	4	12
PREDICTED: unconventional myosin-Ig isoform X1	gi 568970251	2	6

60S ribosomal protein L10	NP_443067.1	5	14
nucleolar protein 56	NP_077155.2	3	8
histone H1.4	NP_056602.1	7	18
heat shock cognate 71 kDa protein	NP_112442.2	14	35
heat shock protein 75 kDa, mitochondrial precursor	NP_080784.1	2	5
splicing factor, proline- and glutamine-rich	NP_076092.1	13	32
stress-70 protein, mitochondrial	NP_034611.2	6	14
heterogeneous nuclear ribonucleoprotein Q isoform 1	NP_062640.2	16	37
40S ribosomal protein S3	NP_036182.1	8	18
DNA-binding protein A long isoform	NP_620817.2	8	18
prohibitin-2	NP_031557.2	4	9
keratin, type I cytoskeletal 14	NP_058654.1	26	58
40S ribosomal protein S4, X isoform	NP_033120.1	9	20
PREDICTED: 40S ribosomal protein S2 isoform X1	gi 568999163	10	22
propionyl-CoA carboxylase beta chain, mitochondrial precursor	NP_080111.1	7	15
60S ribosomal protein L3	NP_038790.2	8	17
heterogeneous nuclear ribonucleoprotein A/B isoform 1	NP_001041526.1	9	18
constitutive coactivator of PPAR-gamma-like protein 1	NP_001028440.2	6	12
superkiller viralicidic activity 2-like 2	NP_082427.1	2	4
PREDICTED: vigilin isoform X1	gi 568908015	2	4
RNA-binding protein EWS	NP_031994.2	2	4
prohibitin	NP_032857.1	2	4
heterogeneous nuclear ribonucleoprotein R isoform a	gi 459683864	28	51
heterogeneous nuclear ribonucleoprotein M isoform b	NP_001103383.1	15	27
RNA-binding protein 39	NP_573505.2	5	9
keratin, type I cytoskeletal 42	NP_997648.2	29	51
splicing factor U2AF 65 kDa subunit isoform 1	NP_001192160.1	3	5
histone H1.2	NP_056601.1	10	16
60S ribosomal protein L13	NP_058018.2	13	20
Friend of PRMT1 protein	NP_075704.2	8	12
40S ribosomal protein S9	NP_084043.1	2	3
nucleolar GTP-binding protein 1	NP_081276.2	2	3
actin, cytoplasmic 1	NP_031419.1	36	53
non-POU domain-containing octamer-binding protein	NP_075633.2	26	38
keratin, type I cytoskeletal 16	NP_032496.1	41	59
keratin, type II cytoskeletal 6A	NP_032502.3	74	106
splicing factor 3B subunit 1	NP_112456.2	5	7
60S ribosomal protein L18	NP_033103.2	5	7
RNA-binding protein Raly short isoform	NP_001132984.1	5	7
desmoplakin	NP_076331.2	8	11
PREDICTED: ATP-dependent RNA helicase A isoform X1	gi 755493774	29	39
junction plakoglobin	NP_034723.1	6	8
galectin-3-binding protein precursor	NP_035280.1	3	4

pre-mRNA-processing-splicing factor 8	NP_619600.2	17	22	
keratin, type I cytoskeletal 17	NP_034793.1	45	58	
methylcrotonoyl-CoA carboxylase subunit alpha, mitochondrial	NP_076133.3	91	116	
keratin, type II cytoskeletal 5	NP_081287.1	163	206	
RecName: Full=Serum albumin; AltName: Full=BSA	P02769.4	12	15	
60S ribosomal protein L19 isoform 1	NP_033104.2	4	5	
nuclease-sensitive element-binding protein 1	NP_035862.2	39	48	
propionyl-CoA carboxylase alpha chain, mitochondrial precursor	NP_659093.2	16	19	
116 kDa U5 small nuclear ribonucleoprotein component isoform b	NP_001103465.1	11	13	
zinc finger RNA-binding protein	NP_035897.2	19	22	
ribonuclease inhibitor isoform a	NP_001165571.1	8	9	
methylcrotonoyl-CoA carboxylase beta chain, mitochondrial	NP_084302.1	10	11	
prelamin-A/C isoform A	NP_001002011.2	21	23	
heterogeneous nuclear ribonucleoproteins C1/C2 isoform 2	NP_001164452.1	13	13	
U5 small nuclear ribonucleoprotein 200 kDa helicase	NP_796188.2	8	8	
transcriptional repressor p66-beta	NP_647465.1	2	2	
interleukin enhancer-binding factor 2	NP_080650.1	39	34	
RecName: Full=Trypsin; Flags: Precursor	P00761.1	59	47	
PREDICTED: interleukin enhancer-binding factor 3 isoform X3	gi 568958887	64	49	
unconventional myosin-IId	NP_796364.2	4	3	
transcription intermediary factor 1-beta	NP_035718.2	4	3	
matrin-3	NP_034901.2	11	7	
PREDICTED: ELAV-like protein 1 isoform X1	gi 568953118	22	7	
PREDICTED: interferon-inducible double-stranded RNA-dependent protein kinase activator A isoform X1	gi 755499566	7	2	
pyruvate carboxylase, mitochondrial isoform 1	NP_001156418.1	2	0	
polypyrimidine tract-binding protein 3 isoform 1	NP_659153.2	2	0	
transcriptional repressor p66 alpha isoform d	gi 557128941	2	0	
DNA topoisomerase 1	NP_033434.2	0	28	
U3 small nucleolar RNA-associated protein 14 homolog A	NP_082552.1	0	4	
PREDICTED: serine/arginine repetitive matrix protein 2 isoform X1	gi 569001949	0	14	
PREDICTED: thyroid hormone receptor-associated protein 3 isoform X1	gi 755508129	0	26	
PREDICTED: chromodomain-helicase-DNA-binding protein 4 isoform X8	gi 568940139	0	4	
dynein heavy chain 9, axonemal	NP_001093103.1	0	2	
DNA ligase 3	NP_034846.2	0	20	
60S ribosomal protein L13a	NP_033464.2	0	5	
bcl-2-associated transcription factor 1 isoform 3	NP_001020564.1	0	22	
serine hydroxymethyltransferase, mitochondrial isoform 2	NP_001239245.1	0	14	
PREDICTED: 60S ribosomal protein L6 isoform X1	gi 568936990	0	15	
serine/arginine-rich splicing factor 1 isoform 1	NP_775550.2	0	19	
60S ribosomal protein L8	NP_036183.1	0	8	
elongation factor 1-alpha 1	NP_034236.2	0	11	
aconitate hydratase, mitochondrial precursor	NP_542364.1	0	7	

glutamate dehydrogenase 1, mitochondrial precursor	NP_032159.1	0	7
ATPase family AAA domain-containing protein 3	NP_849534.2	0	8
PREDICTED: nucleolar transcription factor 1 isoform X3	gi 755538064	0	2
PREDICTED: nuclear mitotic apparatus protein 1 isoform X3	gi 568949281	0	2
tubulin alpha-1B chain	NP_035784.1	0	11
ADP/ATP translocase 2	NP_031477.1	0	6
replication factor C subunit 1	NP_035388.2	0	6
60S acidic ribosomal protein P0	NP_031501.1	0	15
nucleolar protein 58	NP_061356.2	0	7
histone H1.5	NP_064418.1	0	11
arginine-serine-rich splicing factor 6	NP_080775.3	0	4
tubulin beta-5 chain	NP_035785.1	0	11
transmembrane glycoprotein NMB precursor	NP_444340.3	0	10
heterogeneous nuclear ribonucleoprotein D0 isoform a	NP_001070733.1	0	7
TATA-binding protein-associated factor 2N	NP_081703.1	0	4
unconventional myosin-Ic isoform a	NP_001074244.1	0	3
poly(U)-binding-splicing factor PUF60 isoform c	NP_001158072.1	0	6
PREDICTED: ATP-dependent RNA helicase DDX3X isoform X1	gi 569008633	0	7
RRP12-like protein	NP_955518.1	0	3
mitochondrial inner membrane protein isoform 2	NP_001240610.1	0	6
PREDICTED: aminopeptidase N isoform X1	gi 568947434	0	9
PREDICTED: myeloid cell nuclear differentiation antigen-like protein isoform X6	gi 569020023	0	6
PREDICTED: RNA-binding protein 47 isoform X2	gi 568934233	0	4
PREDICTED: 60 kDa heat shock protein, mitochondrial isoform X1	gi 568905803	0	3
PREDICTED: sphingosine-1-phosphate lyase 1 isoform X1	gi 568967055	0	3
trifunctional enzyme subunit alpha, mitochondrial precursor	NP_849209.1	0	7
60S ribosomal protein L14	NP_080250.1	0	8
double-stranded RNA-specific adenosine deaminase isoform 3	NP_001139768.1	0	3
cell division cycle 5-like protein	NP_690023.1	0	11
PREDICTED: splicing factor 3B subunit 3 isoform X1	gi 568955816	0	3
PREDICTED: splicing factor 3B subunit 2 isoform X1	gi 569005837	0	4
<b>FACT complex subunit SPT16 (SUPT16)</b>	<b>NP_291096.2</b>	<b>0</b>	<b>2</b>
transformer-2 protein homolog beta	NP_033212.1	0	7
PREDICTED: 60S ribosomal protein L15 isoform X1	gi 568985566	0	8
serine/arginine-rich splicing factor 5	NP_033185.2	0	8
PREDICTED: H/ACA ribonucleoprotein complex subunit 4 isoform X1	gi 569010120	0	4
PREDICTED: DNA repair protein XRCC1 isoform X1	gi 568945263	0	4
PREDICTED: myelin expression factor 2 isoform X2	gi 568915716	0	6
scaffold attachment factor B2	NP_001025150.2	0	2
PREDICTED: DBIRD complex subunit ZNF326 isoform X1	gi 568936023	0	6
DNA topoisomerase 2-beta	NP_033435.2	0	2
ribosomal L1 domain-containing protein 1	NP_079822.1	0	6

PREDICTED: annexin A2 isoform X1	gi 568960713	0	2	
treacle protein isoform 2	NP_035682.1	0	3	
pre-mRNA-processing factor 6	NP_598462.1	0	3	
leucine-rich PPR motif-containing protein, mitochondrial precursor	NP_082509.2	0	2	
PREDICTED: heterogeneous nuclear ribonucleoprotein H2 isoform X1	gi 569011433	0	6	
putative pre-mRNA-splicing factor ATP-dependent RNA helicase DHX15 isoform 1	NP_001036085.1	0	2	
lamin-B1	NP_034851.2	0	2	
U4/U6.U5 tri-snRNP-associated protein 1	NP_058578.3	0	7	
fragile X mental retardation syndrome-related protein 2	NP_035944.2	0	5	
PREDICTED: apoptotic chromatin condensation inducer in the nucleus isoform X5	gi 568988264	0	3	
PREDICTED: probable ATP-dependent RNA helicase DDX23 isoform X1	gi 568993535	0	4	
heterogeneous nuclear ribonucleoprotein K	NP_079555.1	0	3	
actin-related protein 3	NP_076224.1	0	4	
putative oxidoreductase GLYR1 isoform 1	NP_001073282.1	0	7	
DNA-directed RNA polymerase I subunit RPA34	NP_665821.1	0	2	
RNA-binding protein 25	NP_081625.3	0	2	
lupus La protein homolog	NP_001103615.1	0	3	
PREDICTED: guanine nucleotide-binding protein G(i) subunit alpha-2 isoform X1	gi 568962761	0	2	
sentrin-specific protease 3	NP_109627.3	0	3	
putative ribosomal RNA methyltransferase NOP2	NP_620086.2	0	6	
PREDICTED: glyceraldehyde-3-phosphate dehydrogenase-like isoform 2	XP_001476757.1	0	6	
metastasis-associated protein MTA2	NP_035972.3	0	3	
phenylalanine-tRNA ligase alpha subunit	NP_079924.2	0	2	
serine/arginine repetitive matrix protein 1 isoform 2	NP_001123949.1 (+5)	0	5	
PREDICTED: rho guanine nucleotide exchange factor 2 isoform X7	gi 568921927	0	4	
serine beta-lactamase-like protein LACTB, mitochondrial precursor	NP_109642.1	0	2	
heterogeneous nuclear ribonucleoprotein F	NP_001159902.1	0	8	
<b>SWI/SNF-related matrix-associated actin-dependent regulator of chromatin subfamily A member 5 (SMARCA5)</b>	<b>NP_444354.2</b>	<b>0</b>	<b>4</b>	
RecName: Full=Catalase	P04040.3	0	2	
RNA-binding protein 28	NP_598686.2	0	2	
aspartyl/asparaginyl beta-hydroxylase isoform 3	NP_001171320.1	0	2	
ribosomal RNA processing protein 1 homolog B isoform 1	NP_082520.2	0	5	
PREDICTED: transcriptional activator protein Pur-alpha isoform X1	gi 755560613	0	4	
PREDICTED: fragile X mental retardation syndrome-related protein 1 isoform X4	gi 568920780	0	4	
THO complex subunit 4	NP_035698.1	0	9	
monofunctional C1-tetrahydrofolate synthase, mitochondrial precursor	NP_001164257.1	0	5	
T-complex protein 1 subunit alpha	NP_038714.2	0	3	
histone deacetylase 1	NP_032254.1	0	2	
succinyl-CoA:3-ketoacid coenzyme A transferase 1, mitochondrial precursor	NP_077150.1	0	2	
elongation factor Tu, mitochondrial isoform 1	NP_766333.1	0	2	

zinc finger protein 512	NP_766581.2	0	2
PREDICTED: transformer-2 protein homolog alpha isoform X5	gi 568940051	0	3
PREDICTED: cell growth-regulating nucleolar protein isoform X1	gi 568933825	0	3
endoplasmin precursor	NP_035761.1	0	3
26S proteasome non-ATPase regulatory subunit 2	NP_598862.1	0	3
methyl-CpG-binding domain protein 2	NP_034903.2	0	2
general transcription factor 3C polypeptide 3	NP_001028366.1	0	3
histone H1.1	NP_085112.1	0	11
heat shock protein HSP 90-beta	NP_032328.2	0	4
probable ATP-dependent RNA helicase DDX41	NP_598820.2	0	2
ATP-dependent RNA helicase DDX1	NP_598801.1	0	2
eukaryotic initiation factor 4A-III	NP_619610.1	0	5
cold shock domain-containing protein E1 isoform 1	NP_659150.1	0	2
protein MAK16 homolog	NP_080729.1	0	3
glioma tumor suppressor candidate region gene 2	NP_598592.2	0	2
eukaryotic translation initiation factor 2 subunit 2	NP_080306.1	0	2
PREDICTED: U1 small nuclear ribonucleoprotein 70 kDa isoform X1	gi 568947548	0	2
methyl-CpG-binding protein 2 isoform 1	NP_001075448.1	0	2
tRNA-splicing ligase RtcB homolog	NP_663397.1	0	2
protein KRI1 homolog	NP_663391.2	0	3
ATP-dependent RNA helicase DDX24 isoform 1	NP_001152974.1	0	2
phosphoenolpyruvate carboxykinase [GTP], mitochondrial	NP_083270.1	0	2
ubiquitin-associated protein 2-like isoform 4	NP_001159456.1	0	2
transcriptional activator protein Pur-beta	NP_035351.1	0	3
processing of precursor 1 isoform 2	NP_080616.1	0	2
staphylococcal nuclease domain-containing protein 1	NP_062750.2	0	3
MKI67 FHA domain-interacting nucleolar phosphoprotein	NP_080748.3	0	3
KH domain-containing, RNA-binding, signal transduction-associated protein 1	NP_035447.3	0	4
heterogeneous nuclear ribonucleoprotein A0	NP_084148.1	0	4
PREDICTED: serine/threonine-protein kinase PRP4 homolog isoform X1	gi 568981636	0	2
polyadenylate-binding protein 2	NP_062275.1	0	5
putative RNA-binding protein Luc7-like 2 isoform 2	NP_001164319.1	0	3
glutaminase kidney isoform, mitochondrial isoform 1	NP_001074550.1	0	2
PREDICTED: RNA-binding protein 6 isoform X1	gi 568962788	0	3
succinate dehydrogenase [ubiquinone] flavoprotein subunit, mitochondrial precursor	NP_075770.1	0	2
citrate synthase, mitochondrial precursor	NP_080720.1	0	2
zinc transporter SLC39A7 precursor	NP_032228.2	0	2
PREDICTED: testis-expressed sequence 10 protein isoform X1	gi 568926766	0	4
pre-mRNA 3'-end-processing factor FIP1 isoform 1	NP_001153045.1	0	3
26S protease regulatory subunit 6B	NP_036004.2	0	2
guanine nucleotide-binding protein-like 3-like protein	NP_932778.1	0	2
U2 snRNP-associated SURP motif-containing protein isoform 1	NP_001108449.1	0	2

PREDICTED: C->U-editing enzyme APOBEC-1 isoform X1	gi 568940380	0	2	
PREDICTED: histone lysine demethylase PHF8 isoform X1	gi 569012048	0	2	
PREDICTED: bifunctional polynucleotide phosphatase/kinase isoform X3	gi 568948192	0	2	
regulator of chromosome condensation isoform 1	NP_001184011.1	0	3	
electron transfer flavoprotein subunit alpha, mitochondrial	NP_663590.3	0	6	
U3 small nucleolar RNA-associated protein 18 homolog	NP_001013393.1	0	2	
sequestosome-1	NP_035148.1	0	2	
succinyl-CoA ligase [GDP-forming] subunit beta, mitochondrial precursor	NP_035637.2	0	2	
suppressor of SWI4 1 homolog	NP_663585.2	0	3	
pyruvate dehydrogenase E1 component subunit beta, mitochondrial precursor	NP_077183.1	0	3	
PREDICTED: SAFB-like transcription modulator isoform X4	gi 568961866	0	2	
interferon-induced, double-stranded RNA-activated protein kinase	NP_035293.1	0	2	
calcium/calmodulin-dependent protein kinase type II subunit delta isoform 2	NP_001020609.1	0	2	
RNA-binding protein 7	NP_659197.2	0	2	
small nuclear ribonucleoprotein-associated protein B	NP_033251.1	0	2	
14-3-3 protein zeta/delta isoform 1	NP_001240734.1	0	2	
26S protease regulatory subunit 8	NP_032976.1	0	2	
eukaryotic translation initiation factor 2 subunit 3, X-linked	NP_036140.1	0	2	
lamina-associated polypeptide 2 isoform alpha	NP_035735.2	0	2	
electron transfer flavoprotein subunit beta	NP_080971.2	0	3	
3-hydroxyacyl-CoA dehydrogenase type-2	NP_058043.3	0	5	
isocitrate dehydrogenase [NADP], mitochondrial precursor	NP_766599.2	0	3	
PREDICTED: alpha-enolase isoform X1	gi 755509256	0	3	
40S ribosomal protein SA	NP_035159.3	0	2	
PREDICTED: LOW QUALITY PROTEIN: igE-binding protein-like, partial	gi 755566924	0	2	
PREDICTED: 2'-5'-oligoadenylate synthase-like protein 1 isoform X1	gi 568937127	0	2	
trifunctional enzyme subunit beta, mitochondrial precursor	gi 577019542	0	2	
DNA-directed RNA polymerase I subunit RPA2	NP_033112.2	0	2	
core histone macro-H2A.1 isoform 2	NP_001152985.1 (+5)	0	4	
UPF0568 protein C14orf166 homolog	NP_080804.1	0	2	
caprin-1 isoform b	NP_001104760.1	0	2	
protein TSSC4 isoform 1	NP_064681.1	0	2	
Beta-casein	P02666.2	0	2	
dnaJ homolog subfamily A member 2	NP_062768.1	0	2	
estradiol 17-beta-dehydrogenase 12	NP_062631.1	0	2	
something about silencing protein 10	NP_075541.1	0	2	
F-actin-capping protein subunit beta isoform c	NP_001258334.1	0	2	
DNA-directed RNA polymerase I subunit RPA49 isoform a	gi 551411429	0	2	
DNA-directed RNA polymerases I and III subunit RPAC1	NP_033111.2	0	2	
DNA-directed RNA polymerases I, II, and III subunit RPABC1	NP_079830.2	0	2	
raftlin	NP_852062.1	0	2	
centromere protein V	NP_082724.1	0	2	

elongation factor Ts, mitochondrial precursor

NP\_079813.1

0

2

Complete list of proteins identified by mass spectrometry following RNA pulldown with Mist or Mist-AS probes. Top candidate protein partners for Mist which were screened in follow-up validation experiments are highlighted in yellow. Proteins were identified using peptide thresholds of 90.0% minimum, and protein thresholds of 99.0% minimum and 2 peptides minimum.

## References

1. Wang P, Xu J, Wang Y, Cao X. An interferon-independent lncRNA promotes viral replication by modulating cellular metabolism. *Science*. 2017;358(6366):1051–1055.
2. Ovcharenko I, Nobrega MA, Loots GG, Stubbs L. ECR Browser: A tool for visualizing and accessing data from comparisons of multiple vertebrate genomes. *Nucleic Acids Res*. 2004;32(WEB SERVER ISS.):280–286.
3. Corces MR, Buenrostro JD, Wu B, Greenside PG, Chan SM, Koenig JL, Snyder MP, Pritchard JK, Kundaje A, Greenleaf WJ, Majeti R, Chang HY. Lineage-specific and single-cell chromatin accessibility charts human hematopoiesis and leukemia evolution. *Nat Genet*. 2016;48:1193.

## Major Resources Tables

### **Animals (in vivo studies)**

Species	Vendor or Source	Background Strain	Sex
Mus musculus	The Jackson Laboratory	C57BL/6J	Male

### **Antibodies**

Target antigen	Vendor or Source	Catalog #	Working concentration	Lot # (preferred but not required)
H3K4me3	Millipore	17-614	3µL/ChIP	
PAR	Trevigen	4335-MC-100	ChIP: 1ug/ul	39816F17
PARP1	GeneTex	GTX112864	Native RIP: 1:1500 ChIP: 1ug/ul	41031
PARP1	Abcam	ab227244	Western: 1:2000 Crosslink RIP: 1:250	GR3226439-13
HNRNPA3	Proteintech	25142-1-AP	Western: 1:2000 Native RIP: 1:1000	
SUPT16H	Proteintech	20551-1-AP	Native RIP: 1:500	
SMARCA5	Proteintech	13066-1-AP	Native RIP: 1:500	

### **Cultured Cells**

Name	Vendor or Source	Sex (F, M, or unknown)
RAW 264.7	ATCC, Lot#70000171	Male
THP-1	ATCC	Male